
MCVT: EXTERIOR ENVIRONMENT SUBSYSTEM

METEORITE IMPACT MODEL

AUTHORS: NICHOLAS MASSO, ILIAS BILIONIS

DATE: 12/8/2020

REVISION: 1



Funded by the National Aeronautics and Space Administration under award number 80NSSC19K1076.

Table of Contents

1	Functional Requirements	3
2	Description of the Reference Model Developed	4
2.1	Description of Mathematical Principles	4
2.1.1	Stochastic model of the impact velocity	5
2.1.2	Location, Mass, and Time	8
2.1.3	Crater Sizing	11
2.2	Verification of the reference model	11
2.2.1	Verification	12
2.2.2	Validation	14
3	Modeling Assumptions and Limitations	18
3.1	Assumptions	18
3.2	Limitations	20
4	Model Using Standard Notation	21

Summary

2

Planetary bodies with little or no atmosphere are constantly being hit with meteorites. The properties of the impact environment must be modeled to determine wear on external components of habitat systems. This model is calibrated specifically to the lunar surface and generates random impact events that match with our current understanding of the environment.

4

6

8 **1 Functional Requirements**

The objective of the Meteorite Impact Model is to generate stochastic impact events
10 that match the environment of a given celestial body without atmosphere. The stochastic
events has to include enough information for exciting the affected habitat models.
12 These include the location, time, velocity, and mass of the of the falling object. The frequency
of events and the probability distributions of the important quantities depend
14 on the location. We have restricted our attention to a habitat on the lunar surface.

2 Description of the Reference Model Developed

2.1 Description of Mathematical Principles

16

This model was created for the purpose of simulating the impact environment on the lunar surface. The output of the model is designed to be either generated ahead of time, or generated while running in a Simulink model. The model generates stochastic location, time, mass, and velocity information about impacting bodies, including both sporadic (background) and stream (associated with a meteor shower) events. A function has also been written to find crater size on granular material (like regolith) or solid material depending on density from these parameters. This information is essential for simulating damage on the habitat.

18

20

22

24

There are four primary inputs that define the meteorite external disturbance environment: the area of a rectangular bounding box to be considered, the location of this bounding box on the Moon, the section of time to be considered (implicitly, the duration), and the starting date of the time period. Other factors are completely determined from these inputs or as assumed to be constant.

26

28

The size of the bounding box and the length of time given in the horizon can be used to only query data of interest. The location on the Moon's surface changes the relative vectors of incoming meteoroids, and can even take some sections of the moon out of the path of certain showers due to their radiant point not being correctly aligned to hit those places. The start date of the simulation is needed to account for the rotation of the Moon, and the rotation of the Earth around the Sun, which affect when showers occur and at what angle they impact at.

30

32

34

36

The output of the model is a seven-column array with a number of rows that is equal to the number of sampled impact events. The output template with units is shown in Table 1.

38

Table 1: The desired output from the model and units

x	y	t	m	v_x	v_y	v_z
meters	meters	seconds	grams	km/s	km/s	km/s

As discussed previously, there are four primary characteristics we are concerned about

40

for every impact. The coordinate system is defined in Figure 1 The location of the impact

42 $\mathbf{r} = x\hat{\mathbf{i}} + y\hat{\mathbf{j}}$ (with the coordinate system origin at the bottom left corner of the bounding box), the time the impact occurs t , the mass of the incoming body m , and the velocity

44 it impacts with $\mathbf{v} = v_x\hat{\mathbf{i}} + v_y\hat{\mathbf{j}} + v_z\hat{\mathbf{k}}$ ($\hat{\mathbf{k}}$ points normal to the surface). To sample random events, we have to define the joint probability density function (PDF) $p(\mathbf{r}, t, m, \mathbf{v})$. Note

46 that there is a different joint PDF for steam meteoroids and a each sporadic event. To keep the notational burden to a minimum, we are not going to explicitly show this dependence. The form of the stochastic models we introduce is identical for all cases –

48 only the parameters differ.

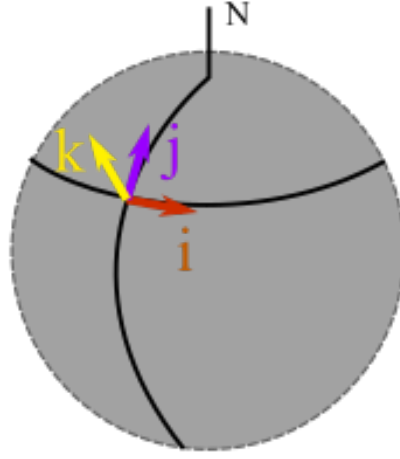


Figure 1: Image of the lunar Surface reference frame. Note how $\hat{\mathbf{j}}$ is pointing directly north, $\hat{\mathbf{i}}$ is pointing east, and $\hat{\mathbf{k}}$ is normal to the surface.

50 2.1.1 Stochastic model of the impact velocity

The first assumption we make is that the magnitude of the velocity is independent of any

52 other properties of the meteorite. This allows breaking the joint PDF into Equation 1.

$$p(\mathbf{r}, t, m, \mathbf{v}) = p(\mathbf{r}, t, m) p(\mathbf{v}). \quad (1)$$

The velocity is a three-dimensional vector represented as:

$$\mathbf{v} = v_s(u_1\hat{\mathbf{i}} + u_2\hat{\mathbf{j}} + u_3\hat{\mathbf{k}}), \quad (2)$$

where v_s is the speed, and $\hat{\mathbf{u}} = u_1\hat{\mathbf{i}} + u_2\hat{\mathbf{j}} + u_3\hat{\mathbf{k}}$ is a unit vector. We further assume that impact speed is independent of the direction, i.e., 54

$$p(\mathbf{v}) = p(v_s)p(\hat{\mathbf{u}}). \quad (3)$$

Given the average speed \bar{v}_s for both sporadic (about 17 km/s) and stream meteoroids (varies). Since v_s is a positive parameter, we assign an Exponential distribution to it with rate \bar{v}_s^{-1} [5]. The rationale behind this choice is that the Exponential maximizes the entropy subject to the available constraints. We write: 56
58

$$v_s \sim \text{Exponential}(\bar{v}_s^{-1}). \quad (4)$$

For the direction, we assume that $u_3 < 0$, so that we are only sampling directions that hit the surface (these are the only ones we have observations for anyway), and u_1 and u_2 can be arbitrary. A simple model is to define the random variables: 60
62

$$\begin{aligned} u'_1 &\sim U([-1, 1]), \\ u'_2 &\sim U([-1, 1]), \\ u'_3 &\sim U([-2, 0]), \end{aligned}$$

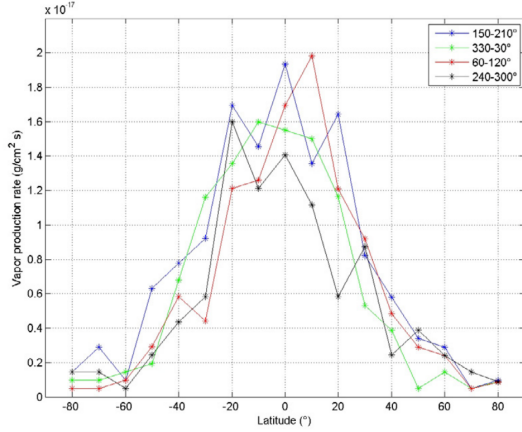
and then set:

$$\begin{aligned} u_1 &= \frac{u'_1}{u'_1 + u'_2 + u'_3}, \\ u_2 &= \frac{u'_2}{u'_1 + u'_2 + u'_3}, \\ u_3 &= \frac{u'_3}{u'_1 + u'_2 + u'_3}. \end{aligned}$$

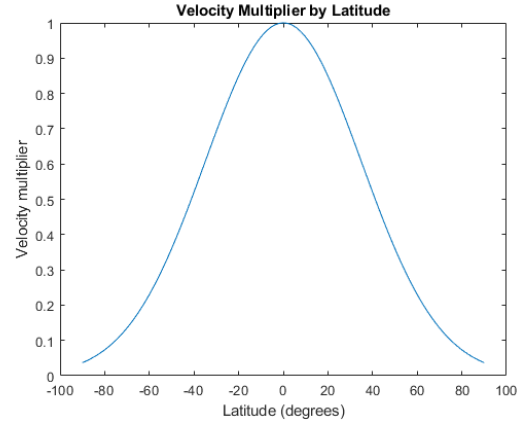
Now, it is known that impacts on the lunar surface are more violent near the equator [2]. This is due to a large number of impactors originating from main belt asteroids. In any case, the velocity of the vector must be corrected to adjust for this effect. To this end, we take into account the vapor production rate vs latitude λ data given in Cremonese et al, see Fig. 2a. We assume that the observed vapor production rate is directly correlated 64
66
68

to the impact speed at a given latitude. The assumption is that the impact velocity will
 70 scale proportionally to the vapor production rate. To capture this effect, we construct a
 bell curve to serve as a multiplicative factor $s_{\text{lat}}(\lambda)$ of the impact speed. Then, the speed
 72 can then be represented as:

$$v_{\text{corrected}} = s_{\text{lat}}(\lambda) v_s. \quad (5)$$



(a) Vapor production by latitude from [2]



(b) Approximated velocity by latitude

Figure 2: Comparison of velocity multiplier approximation with data.

The equations discussed thus far are not applicable to meteor showers, where there are
 74 known sub-radiant points for all of the streams. The sub-radiant point is the location on
 the celestial sphere where the objects originate from, which is also used to name them
 76 based on what constellation this point is near. This point, along with the knowledge of
 average velocity for each shower, defines the vectors completely.

78 The normal vector on the Moon's surface at the location being evaluated, $\hat{\mathbf{k}}$, can be rep-
 resented as a unit Z component on a rectangular system with the y axis pointing towards
 80 the north pole. See Figure 1. This coordinate system is in motion, and changes as the
 Moon and Earth revolve around the Sun. The celestial sphere is fixed relative to the sun.
 82 The vector the meteors approach from $\hat{\mathbf{u}}_{\text{stream}}$ is a unit vector that can be represented
 as the negative of the vector pointing towards the point on the celestial sphere from the
 84 sun.

A coordinate transformation can be applied to find the vector of the meteors relative to
 86 the surface of the moon in the frame defined by normal $\hat{\mathbf{k}}$. The 3-2-1 Euler matrix using

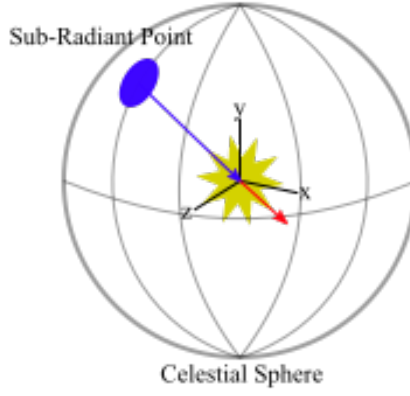


Figure 3: Definition of celestial vector system. The blue vector shows the direction of a meteor as if it were approaching, and the red vector shows the vector in the reference frame.

the surface frame is defined as \mathbf{E} , and the relative meteor vector $\hat{\mathbf{u}}_{\text{rel}}$ is defined by:

$$\hat{\mathbf{u}}_{\text{rel}} = \mathbf{E}\hat{\mathbf{u}}_{\text{stream}} \quad (6)$$

At this point, it is possible to determine if the surface can actually be hit by this meteor. 88
This is a simple matter and can be done by checking if $\hat{\mathbf{k}}$ is negative. If not, the location 90
on the surface must be facing away from the sub-radiant point, and is being blocked by 90
the other side of the moon. These events are simply ignored. If the impact is feasible, the 92
true velocity vector is then calculated by multiplying $\hat{\mathbf{u}}_{\text{rel}}$ by the known mean velocity of 92
the stream, v_{stream} . There is no correcting factor for the latitude applied.

$$\mathbf{v} = \bar{v}_{\text{stream}}\mathbf{u}_{\text{rel}} \quad (7)$$

2.1.2 Location, Mass, and Time 94

Now let us return to $p(\mathbf{r}, t, m)$. First, assume that \mathbf{r} varies within a small region of area 96
 A where the latitude λ can be assume to be constant. This assumption is validated in 96
a later section. For sporadic meteorites, the probability is not dependent on any time 98
factors. Therefore, $p(\mathbf{r}, t, m)$ should only be a function of m . We can assume that the 98
probability of finding a meteorite within a given area A and a given time interval Δt and 100
any mass in $(0, +\infty)$ is a Poisson process with known rate $N(m)$. This rate is the mass flux

at the Moon's surface, in $\text{s}^{-1} \text{m}^{-2}$. The primary equation for the mass-flux relationship is:

$$\log_{10}(N) = \begin{cases} \sum_{n=0}^6 a_n (\log_{10}(m))^n, & \text{if } x \leq 1000, \\ -15.42 - 0.8 \log_{10}(m), & \text{otherwise,} \end{cases} \quad (8)$$

102 where N is the flux, and m is the mass.

Table 2: Parameters for polynomial in Equation 8

a0	-14.711
a1	-1.3466
a2	0.0247
a3	0.0045
a4	-0.0014
a5	-0.0002
a6	-0.000005

This equation was derived from two models. The sub-kilogram relationship was derived
104 from raw flux at different masses provided in Grün's 1985 paper [4]. Grün provides discrete flux values at different masses, but generating values is more efficient with a continuous function. A polynomial was fit to these values using MATLAB's polyfit function.
106 These values are in Table 2. Above one kilogram, Dycus proposes a flux relationship that
108 is valid for most locations in the solar system [3]. Dycus's original model is:

$$\log(N) = -18.97 + 4.44r - 0.89r^2 - 0.8 \log(m), \quad (9)$$

where r is the distance of the body from the sun in Astronomical Units, and m is the
110 mass in grams. Only one body at a consistent radius from the Sun is being observed, so
it is possible to replace r with a constant. A value of $r = 1$ is appropriate as the moon's
112 orbit distance is roughly 0.0026 AU from Earth, a fraction of a percent variance over the
course of a month. This leaves the simplified equation seen in Equation 8.

114 To find the total number of impact events that are likely to happen, we apply the Poisson
distribution to the product of A , Δt , and the total mass flux. It is worth noting that the
116 integral of $N(m)$ does not actually converge at ∞ , and a reasonable upper bound must

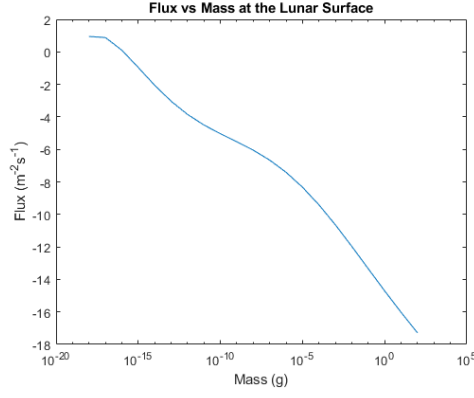


Figure 4: Flux - mass relationship on the Moon's surface.

be chosen. This is addressed in the assumptions.

$$n_{\text{events}} = \text{Poisson} \left(A \Delta t \int_0^{\infty} N(m) dm \right) \quad (10)$$

The units of $A = m^2$, $\Delta t = s$, and $N(m)dm = s^{-1}m^{-2}$ cancel appropriately for a non-dimensional Poisson parameter. 118

Once the total number of impacts is known, the spatial and time coordinates are sampled uniformly (within the bounding box and the time period under consideration respectively). To sample the masses of each event, we use a rejection sampling algorithm [1]. 120 122

To apply this process for stream meteorites, the rate is now dependent on orbital position. This can be turned into a function of time via the start date. The approximation in this model uses a piece-wise function for two sections of the shower, for low intensity and high intensity. These correspond to two different flux scaling factors, σ_l and σ_h . These are scaled by the shower's known Zenithal Hourly Rate (ZHR) compared to the ZHR of sporadic meteorites. 124 126 128

The total time is integrated, and the same Poisson process is simulated. This time the integral of mass flux is scaled by each sigma, $\int_0^{\infty} \sigma F(m) dm$. It is important to note that our equation for $F(m)$ is logarithmic, so the scaling has to be applied to the linear version of the equation. The values for these showers were found in Melosh's paper on shower rates [6]. 130 132 134

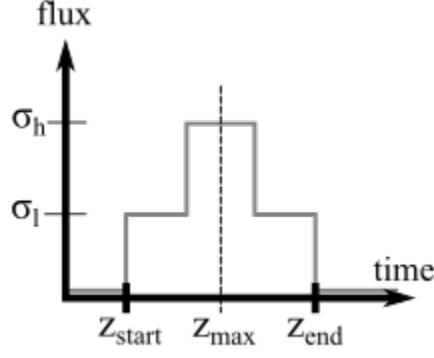


Figure 5: Representation of the model approximation for shower flux over time.

2.1.3 Crater Sizing

136 With the parameters known from the $p(x, t, m, v)$ sample, the crater sizing formula from
[6] can be applied. These equations hold for craters smaller than 100m in diameter. The
138 information from the densities is used in these formulae, shown below. There are two
cratering relationships, one in solid material and another into granular material. Melosh
140 generalized these equations for many types of impact surfaces with different densities,
but they are most accurate for the lunar surface on regolith.

$$d_{c,granular} = 0.25 \rho_p^{1/6} g_M^{-1/2} g_M^{-0.165} E_{kin,p}^{0.29} \sin^{1/3}(\theta) \quad (11)$$

$$d_{c,solid} = 0.015 \rho_p^{1/6} g_M^{-1/2} g_M^{-0.165} E_{kin,p}^{0.37} \sin^{2/3}(\theta) \quad (12)$$

d_c	crater diameter (m)
ρ_m	impacted body density (g/cm^3)
g_m	gravitational acceleration (m/s^2)
θ	impact angle from horizontal
ρ_p	projectile density (g/cm^3)
$E_{kin,p}$	projectile kinetic energy (J)

Table 3: List of parameters for Equation 11 and 12

142 2.2 Verification of the reference model

For this model to be accepted, it must both be verified and validated. To verify the
144 model, we examine a synthetic example output and make sure it satisfies the needs of

the model. To validate the model, this output data can be compared against real observed data from the lunar surface.

146

2.2.1 Verification

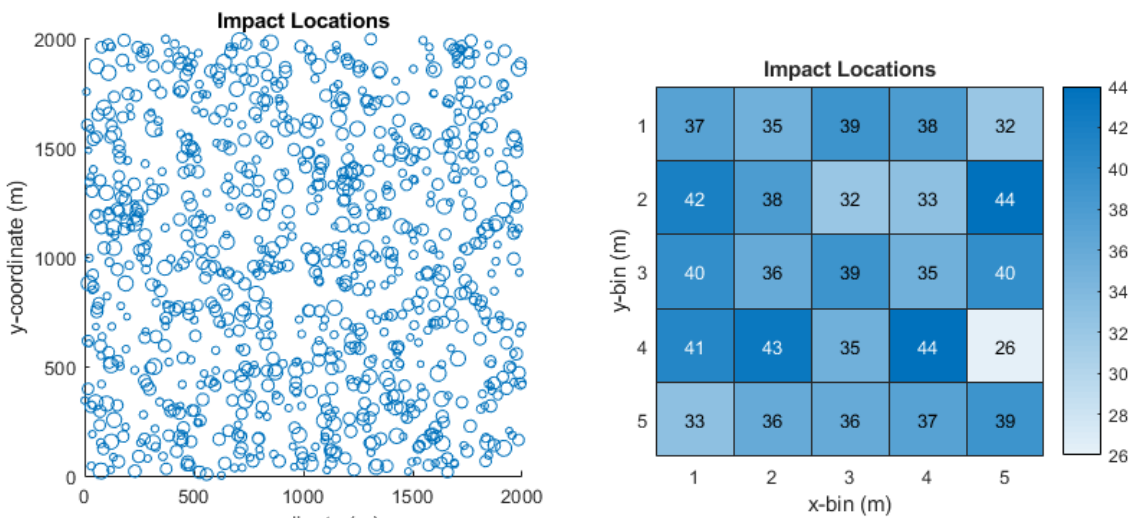
The output of this model, defined in Table 1, can be verified by checking each component logically. An example data set will be generated, "observing" an area 2km square on the lunar equator for five years. The first parameter is the location of each impact. This should be purely random, and is generated directly from a uniform distribution. By looking at Figure 6a one can get an idea of all the impacts, but it is hard to validate the distribution is uniform. By breaking the surface into chunks, we can compare the number of impacts per chunk more easily.

148

150

152

154



(a) Scatter plot of impact location. Marker size corresponds to velocity.

(b) Same impacts, sorted into 25 bins.

Figure 6: Impact locations on x-y plane.

Three runs of the same time period generate very slight differences in the output data, as shown in Figure 7. Different areas have relatively more impacts, but these areas change randomly and the total number and average location do not change significantly.

156

To verify the time spread of the impacts, we can look at a histogram of all impacts in the five year period. Figure 8 shows the cyclical repetition of each year in this period. To get a closer look, Figure 9 shows a single year of this period. It is possible to distinguish the spikes in rate for each of the major showers; the overlap of the SDA and Perseids in the spring, the Geminids in the fall, and then the Quadrantids as winter begins. These

158

160

162

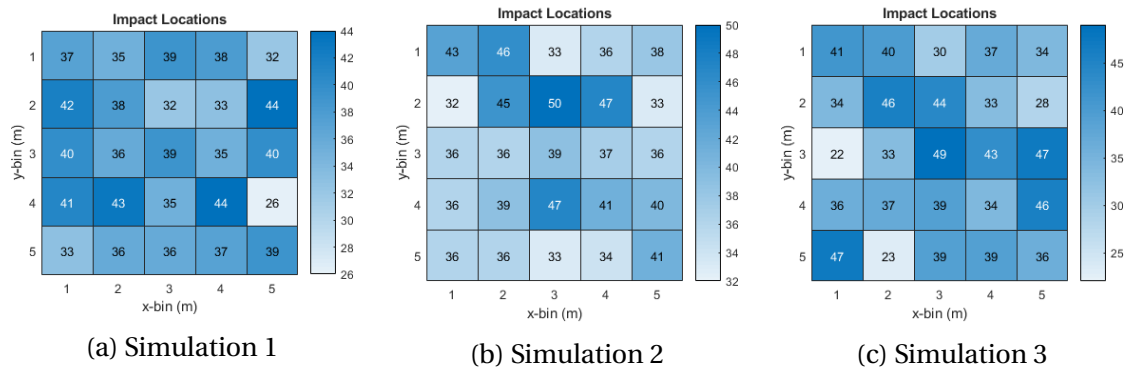


Figure 7: Three separate simulations of the same time period.

correspond correctly to the times of year on Earth when these showers occur.

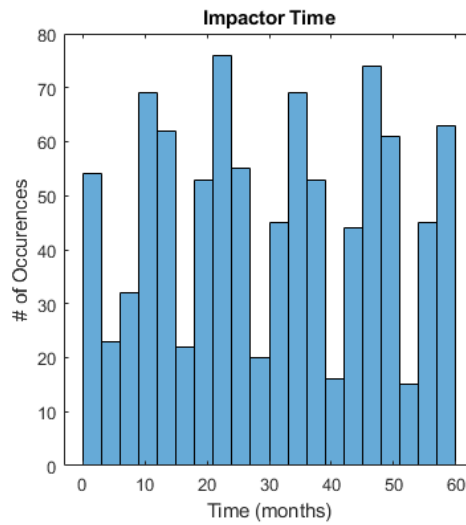


Figure 8: Histogram of impact events over 5-year period.

The mass distribution shown in Figure 10 lines up cleanly with our distribution from Equation 10. However, more informative analysis can be performed when comparing this to real data, in the Validation section.

The velocities are rather well defined, and at the equator, we can see the results from the same five-year simulation in Figure 11. All sporadic impacts are centered in the 16-24 km/s range, while the stream values are set at their known velocities. To verify the vectors are logical, we can plot the velocity along the surface in Figure 11b. Sporadic impacts are centered around zero, while the stream impacts are along straight lines that correspond to where the moon is oriented. The vector transformation is verified here, as the orientation of the vectors does not change in the y-direction on the equator.

To verify the velocity model holds while changing latitudes, the same 2km-square simulation can be done at a location 45 degrees north of the first simulation. This causes

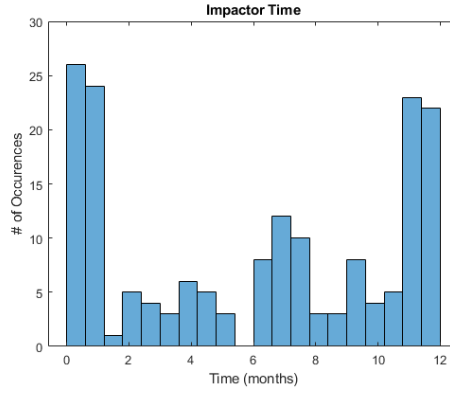


Figure 9: Histogram of impact events over 1-year period. Starts on January first.

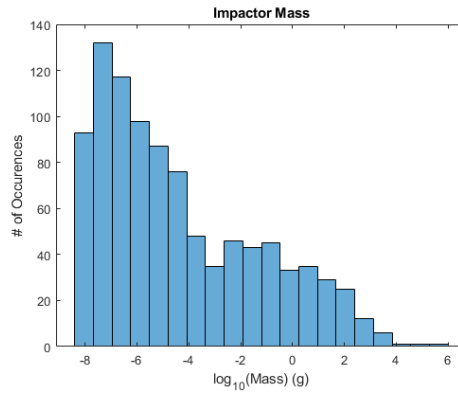


Figure 10: Histogram of masses generated by model on log scale.

the sporadic velocities to be slightly slower, and the stream velocities to be constant in 176
Figure 12a. The orientation of these vectors changes more as the moon rotates, shown
in Figure 12b. Impacts from below the celestial equator, such as in the Southern Delta 178
Aquariids, have high components of the velocity in the x-y plane, meaning they are just
glancing the surface. These observations verify the model is adjusting for latitude prop- 180
erly.

2.2.2 Validation 182

To determine the accuracy of the exterior environment model, the output can be com-
pared to studies of the impact environment on the lunar surface. 184

A comparison was made to the NELIOTA study of lunar impacts [5]. This study had an
Earth-based telescope watch a section of the lunar surface for impact flashes, and then 186
used the magnitude of the flash at various wavelengths to determine impact energy. Us-
ing known average velocities, the mass of the impacting bodies are able to be estimated. 188
The area covered by the telescope is estimated at $3.11 * 10^6 km^2$ and the total duration

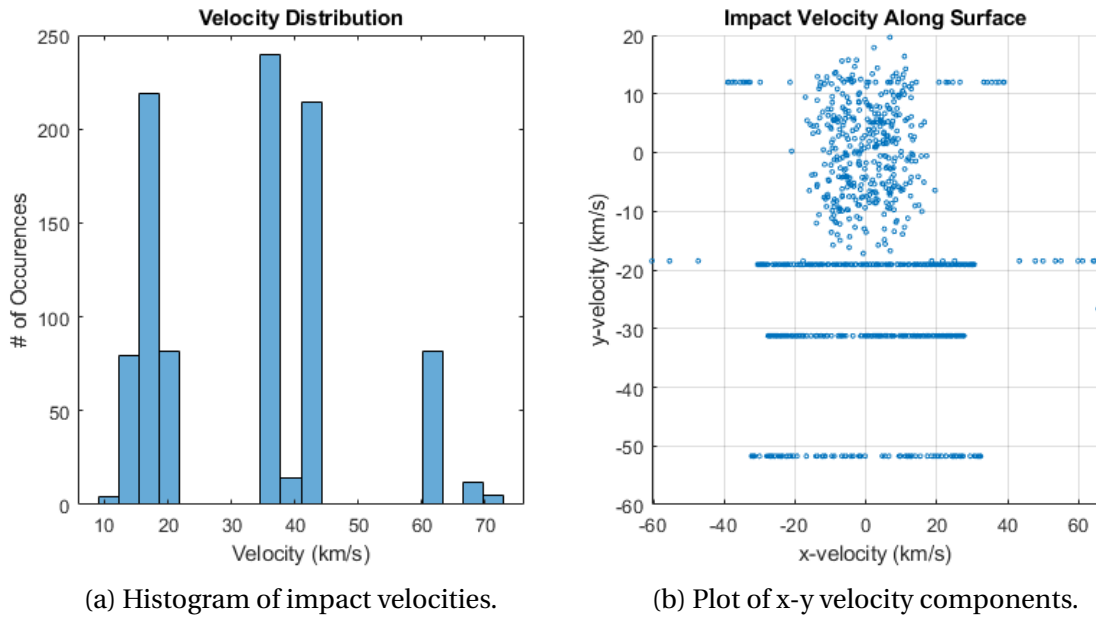


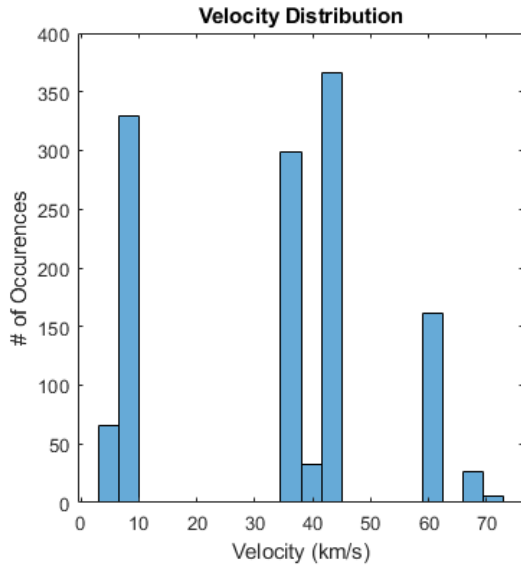
Figure 11: Velocity distribution at the equator.

190 was 110.48 hours. These can be set as inputs to the model, and an output data set created.

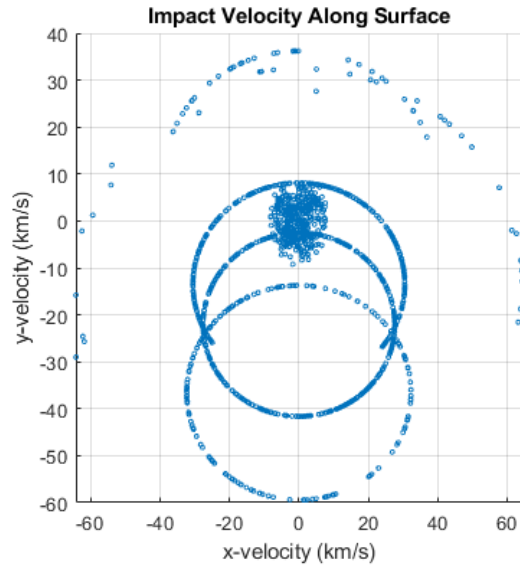
192 The NELIOTA study could only detect flashes above a certain magnitude, which set a lower bound of around 100g for meteorite mass. The histogram of impact masses generated can be cut off at this value to match the scales of the graphs. Both histograms are compared in Figure 13.

196 The model has been tuned so that the upper end of generated impacts matches near the available data in this study. This ensures that masses here are appropriately frequent and represented in the data set. These are the more important impacts, and will have the most influence on other sections of the model. Comparing exactly to the study's time of observing is difficult, as the model operates within a short continuous time, while the study operated over several years for short observing periods. This leads to a possible bias towards stream meteorites, as it was common that observing times aligned with high intensity meteor showers. When the model simulates during a stream, the number of impacts can exceed the number presented in the NELIOTA study. Other simulations generate fewer impacts.

206 The mean number of impacts above 100 grams generated by 12 different runs of the model (one in each month) is 64. Maximum impacts generated is 121, minimum is 34. These can be compared to NELIOTA's 112 impacts observed in this period. These



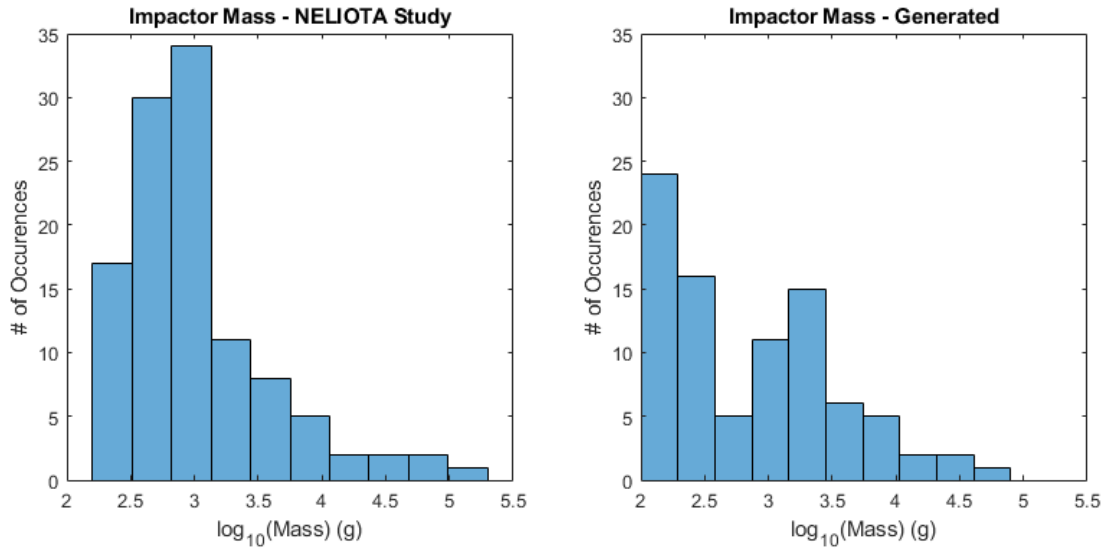
(a) Histogram of impact velocities.



(b) Plot of x-y velocity components.

Figure 12: Velocity distribution at latitude 45 degrees north.

conclusions validate the higher mass values produced by the model as close approximations.



(a) Histogram of impact masses estimated by the NELIOTA team. (b) Histogram of impact masses generated by the model.

Figure 13: Comparison of upper-end impact masses generated by the model to observed data.

3 Modeling Assumptions and Limitations

3.1 Assumptions

This model has several assumptions built-in that are necessary to generate results based on our current understanding of the Moon's impact environment. These can be changed in the future, but for now give a reasonable approximation of the conditions at the surface.

The first assumption lies with in the function for mass flux, $F(m)$. The integral does not converge to infinity. The second integrating the second equation for $1000 < m < \infty$ is:

$$\int_{1000}^{\infty} N = \int_{1000}^{\infty} 10^{-15.42-0.8\log_{10}(m)} dm \quad (13)$$

This becomes:

$$\Delta N = \int_{1000}^{\infty} 10^{-15.42} + m^{-0.8} dm \quad (14)$$

And ends as:

$$\Delta N = 10^{-15.42}m + m^{0.2} \Big|_{1000}^{\infty} = \infty \quad (15)$$

MATLAB picks a large value to approximate infinity at, but a large value can be chosen for additional control. This value does not matter as much, as this is one of two scaling factors available for calibrating the model. I have selected 10^{24} grams, as this is one order of magnitude smaller than the total mass of the Moon [7]. The second scaling factor is applied the same way as the scaling factor σ given to $F(m)$ in the shower sections.

Another assumption made here is that velocity is a completely independent factor for the Poisson process, and is not dependent on anything else other than the origin of the meteorite, and the latitude the impact occurs at (for sporadic impacts only). This may be erroneous, and velocity may be coupled to direction. However, this is not covered in any research papers reviewed thus far, and has been deemed insignificant.

As the program is currently implemented, the area evaluated for impacts is treated as a flat plane. This leads to an issue when the area grows so big that the latitude and

longitude change inside the area. The length along the surface d by degree change θ is
234 simply a radians to degrees conversion with the Moon's radius R_m :

$$\theta = d \left(\frac{360}{2\pi R_m} \right) \quad (16)$$

A 0.5 degree change in latitude or longitude is equivalent to a 30.3 km distance along the
236 Moon's surface. The flat assumption is perfectly valid for the distances we are working
with that are under 1 km. If analysis must be performed at larger scales, the area can be
238 broken up into several rectangles with different latitude and longitude values.

Another assumption made is that both the Earth and Moon have perfectly circular and
240 in-plane orbits. This is made to simplify the calculations of position around the sun/-
surface vectors on the moon to avoid using a true physics model of the Solar System, re-
242 ducing computational time dramatically. This also allows for plugging in a single value
for the Moon's distance for the sun in the second half of the Flux equation. The celes-
244 tial equator is defined along the plane of Earth's orbit, so this is perfectly valid. The
eccentricity of the earths orbit is 0.017, which leaves a 3.35% change in orbital distance
246 through the year. Mean orbital distance is used in the model, as well as the true orbit
time.

248 The Moon's orbit has an eccentricity of 0.0549, which results in a 10.98% change in or-
bital distance to the Earth over a month, but this also changes over the course of an
250 Earth year. The important factor, distance to the sun, changes at maximum of 0.27%
over the course of a month. This distance change is insignificant to the calculation of
252 mass flux. The orbit is inclined at 5.145 degrees from the ecliptic, and the moon has an
obliquity of 6.68 degrees. This might be a factor worth accounting for in later versions of
254 the program, as a vector at the north pole of the moon could be as much as 11 degrees
away from its calculated value. However, this is only important for stream meteorites,
256 as the sporadic meteorites (the bulk of values) are randomly distributed vectors.

The moon is assumed to be perfectly spherical in this model. This makes for very simply
258 surface normal vector calculations. The moon has an ellipticity (flattening) value of
0.0012, aka the polar radius is 0.12% smaller than the equatorial radius. This is the fifth
260 most spherical planetary body in the solar system, and can be approximated well as a
perfect sphere.

3.2 Limitations

262

This model has a set of limitations that are intrinsic to the set of assumptions made while creating it. These do not have a large effect on the current setup, but changing requirements in the future might require changes to the model. 264

The first limitation is that dust generated specifically by these impacts is not evaluated in this model. All dust calculations are made by a different model system, but these two sections of the environment are linked. A more realistic model would use perhaps the output of this impact model to generate the dust environment. 266 268

A limitation brought on by an assumption made is that large areas (greater than 30km per side) cannot be processed accurately in a single run of the model. Multiple iterations must be done with different parameters to reflect changing latitude and longitude. As mentioned in the assumptions section, this is only a consideration when the area under consideration is larger than 30 km in any direction. If large-scale studies of the lunar impact environment is being considered, computational time might become an issue, and considering this scenario would require a change in the model's architecture. 270 272 274 276

The current model only handles rectangular areas. This keeps things simple inside the program, and other parts of the habitat model would know whatever locations they are at and poll the impacts. This might be inefficient, as small habitats might cover a large area but only have bodies at certain locations, but this is currently an acceptable inefficiency and does not add much computational time for areas less than a kilometer in side length. 278 280 282

Another limitation is that lunar geography is completely ignored in this model. If a habitat is being considered near a large impact crater, or a valley or mountain on the surface, this model does not take into account the shielding provided. This would be an incredibly difficult task to accomplish for the entire moon, and later a function could be implemented that removes impact events with vectors and locations that would be blocked by surrounding terrain. 284 286 288

4 Model Using Standard Notation

290 The Exterior Environment Model receives no input from other systems/sub-systems.
 This model uses the given start date, latitude and longitude, and area before beginning
 292 the simulation. After the simulation is started, it can output values to the other systems
 of the habitat. This model is not currently integrated with other subsystems, but the
 294 primary point of interaction would be with the Structural Model, and perhaps the power
 generation model if impacts change power output. The set of standard notations used
 296 for this model is as seen in Table 4.

Table 4: Standard Notations for Meteorite Impact Model

Categories	Standard Notation	Variable	Description
9*Parameters	Θ_1	x_0	starting x-coordinate of bounding box
	Θ_2	x_1	final x-coordinate of bounding box
	Θ_3	y_0	starting y-coordinate of bounding box
	Θ_4	y_1	final y-coordinate of bounding box
	Θ_5	t_0	Start time of current horizon
	Θ_6	t_1	End time of current horizon
	Θ_7	Θ	local longitude
	Θ_8	λ	local latitude
	Θ_9	d	start date of simulation
7*Outputs	Y_1	x	x-location of impact event
	Y_2	y	y-location of impact event
	Y_3	t	time of impact event
	Y_4	m	mass of impacting body
	Y_5	v_x	x-component of velocity
	Y_6	v_y	y-component of velocity
	Y_7	v_z	z-component of velocity

References

- [1] George Casella, Christian P. Robert, and Martin T. Wells. *Generalized Accept-Reject sampling schemes*, volume Volume 45 of *Lecture Notes–Monograph Series*, pages 342–347. Institute of Mathematical Statistics, Beachwood, Ohio, USA, 2004. 298
- [2] G. Cremonese, P. Borin, A. Lucchetti, F. Marzari, and M. Bruno. Micrometeoroids flux on the Moon. *Astronomy & Astrophysics*, 551:A27, March 2013. 300
- [3] Robert Dycus. The Meteorite Flux at the Surface of Mars. *Astronomical Society of the Pacific*, 1969. 302
- [4] E. Grün, H.A. Zook, H. Fechtig, and R.H. Giese. Collisional balance of the meteoritic complex. *Icarus*, 62(2):244–272, May 1985. 304
- [5] Alexios Liakos, Alceste Bonanos, Emmanouil Xilouris, Detlef Koschny, Ioannis Bellas-Velidis, Panayotis Boumis, Vassilios Charmandaris, Anastasios Dapergolas, Anastasios Fytsilis, Athanassios Maroussis, and Richard Moissl. NELIOTA: Methods, statistics and results for meteoroids impacting the Moon. *Astronomy & Astrophysics*, 633:A112, January 2020. arXiv: 1911.06101. 306
- [6] H. J. Melosh. Impact cratering. a geologic process. *Geological Magazine*, 126(6):729–730, 1989. 308
- [7] D. R. Williams. Moon fact sheet. <https://nssdc.gsfc.nasa.gov/planetary/factsheet/moonfact.html>, 2020. Accessed Oct 3, 2020. 310